

Generalized Space Vector Pulse Width Modulation Technique for Cascaded Multilevel Inverters

Xiaodong Yang, Chonglin Wang, Liping Shi and Zhenglong Xia

*School of Information and Electrical Engineering,
China University of Mining and Technology, Xuzhou, Jiangsu 221116, China
24661883@qq.com*

Abstract

In this study, a generalized space vector pulse width modulation (SVPWM) method is proposed for cascaded H-bridge multilevel inverters. An explicit modulation function expression of the generalized SVPWM method is established for a single-stage cascaded inverter. Various continuous SVPWM and discontinuous PWM methods are obtained easily by changing the zero vector distribution coefficient. The generalized SVPWM method for cascaded multilevel inverters is achieved via the carrier phase shift strategy. A simple digital realization method for the generalized SVPWM is also proposed. By using this method, complex trigonometric function calculations, coordinate transformations, space vector selections, and duration time calculations are avoided. Finally, the simulation model and experimental device of the eight cascaded multilevel inverters are built to test the proposed method. The harmonic characteristics of the different modulation method are also analyzed. Simulation and experimental results demonstrate the feasibility and effectiveness of the method.

Keywords: *Cascaded multilevel inverter, H-bridge, Generalized SVPWM, DPWM*

1. Introduction

Cascaded H-bridge multilevel inverters are widely used in motor control, reactive compensation, and harmonic suppression because of their advantages such as modularity, high power capacity, good harmonic characteristic, and easily realized redundancy.

Two strategies in pulse width modulation (PWM) control are generally used: (1) sine PWM (SPWM), which is based on the carrier [1, 2]; and (2) space vector PWM (SVPWM) [3, 4]. Each method has its own advantages and disadvantages and is suitable for different occasions. SPWM is simple and easy to implement. This method can be divided into carrier disposition PWM and phase shift carrier PWM. SVPWM has the highest voltage utilization ratio and is developed from the magnetic flux trajectory control in the speed control of an AC motor. Discontinuous SVPWM (DPWM) methods can be obtained by changing the distribution of the zero vectors through different strategies [5, 6]. DPWM has attracted significant attention because this method minimizes switch loss [7].

The generalized SVPWM method is obtained by studying the inner links of different DPWM methods. Numerous scholars have established the explicit modulation function expression in three-phase bridge voltage source inverters [8-10]. The numbers of voltage vector and switching state for cascaded multilevel inverters rapidly increases with increasing

cascaded number N . If the cascaded number is more than 2, then the SVPWM method becomes extremely complex and difficult to achieve. As a solution to practical applications, the two-level SVPWM method is used for the first single-stage inverter, and then, the PWM control of the rest of the subunits are obtained via the carrier phase shift method [11-13]. In this paper, the cascaded H-bridge multilevel inverter and its generalized SVPWM method are discussed.

2. Realizing Generalized SVPWM

The single-stage structure of cascaded inverters is presented in Figure 1. A multilevel cascaded inverter is composed of N series single-stage subunits, which generally form a neutral common point that uses the star connection scheme on one side and is connected to the grid through the reactor on the other side.

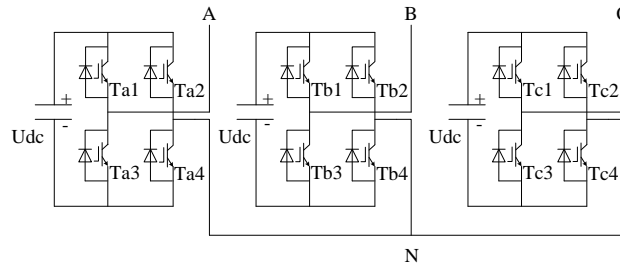


Figure 1. A single-stage structure cascaded inverter

2.1. The generalized SVPWM modulation function of a single-stage inverter

In a single-stage structure (Figure 1), the state of each bridge arm is indicated by the switching state of the upper tube, such as (L_a, L_b, L_c) or (R_a, R_b, R_c) . The eight basic voltage space vectors are obtained through different combinations of the switching state of the left bridge arm. Each vector can be expressed as

$$V_L = \frac{2U_{dc}}{3} (L_a + L_b e^{j\frac{2}{3}\pi} + L_c e^{-j\frac{2}{3}\pi}) \quad (1)$$

A two-level space vector consists of the states of the three left or right bridge arms, which are the left bridge arm voltage vector $V_L(L_a, L_b, L_c)$ and the right bridge arm voltage vector $V_R(R_a, R_b, R_c)$. As shown in Figure 2, the voltage vector of a single-stage inverter can be expressed as

$$V = V_L - V_R. \quad (2)$$

We generally consider V_L and V_R with equal amplitude and opposite phase to obtain the maximum output voltage. Therefore, we can determine that voltage vector V has the same phase and double the amplitude of V_L .

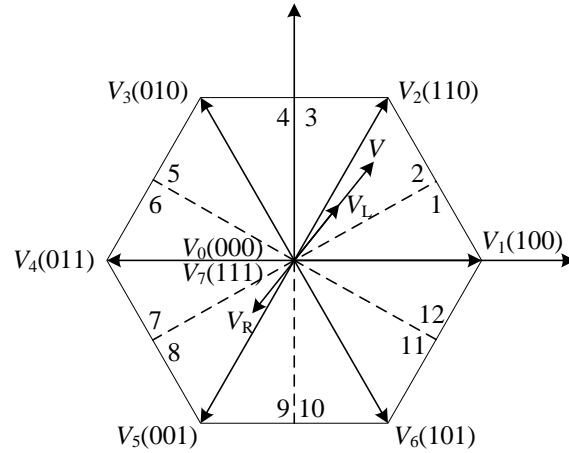


Figure 2. Voltage space vectors

In this study, the traditional 6 sectors are divided into 12 sectors (Figure 2) for a simple and convenient analysis of different DPWM methods.

The generalized SVPWM method is used to determine a three-phase reference voltage waveform. We can obtain the PWM waveform, which is identical to the PWM waveform based on the SVPWM method, by comparing the waveform with a triangular wave.

For example, the left bridge arm voltage vector V_L in the second sector has four basic vectors V_1 , V_2 , V_0 , and V_7 . The duration time of V_1 and V_2 are T_1 and T_2 , respectively, which can be calculated by using the voltage-second balance principle. The duration time of zero vectors V_0 and V_7 are t_0 and t_7 , respectively, which can be expressed as

$$\begin{cases} t_7 = kT_0 \\ t_0 = (1-k)T_0 \\ T_0 = T_s - T_1 - T_2 \end{cases}, \quad (3)$$

where T_s is the switching cycle, T_0 is the total time of the zero vector, and k is the zero vector distribution coefficient.

Different PWM methods can be obtained when k has different values. When $0 < k < 1$, zero vectors V_0 and V_7 are involved in an arbitrary voltage vector called continuous SVPWM (CPWM). When $k=0.5$, SVPWM is the most commonly used approach. If the resultant voltage vector fixed select zero vector V_0 or V_7 or select different zero vectors in different sectors, then discontinuous SVPWM (DPWM) is employed. DPWM can determine if the bridge arm switch is inactive at a certain interval in each cycle, and thus, it can reduce switching frequency and switching loss. DPWM can be divided into the following methods based on different zero vector distributions.

DPWMmax: V_7 is fixed selected as the zero vector, which can determine the inactive switches of the left and right bridge arms in a 120° interval in the positive half cycle of the output voltage.

DPWMmin: V_0 is fixed selected as the zero vector, which can determine the inactive switches of the left and right bridge arms in a 120° interval in the negative half cycle of the output voltage.

DPWM0: V_0 is selected in Sectors 1, 2, 5, 6, 9, and 10. V_7 is selected in the remaining sectors. These vectors determine the inactive switches of the left and right bridge arms in a 60° interval in the positive and negative half cycles of the output voltage. The inactive interval is 30° ahead of the voltage peak.

DPWM2: V_7 is selected in Sectors 1, 2, 5, 6, 9, and 10. V_0 is selected in the remaining sectors. These vectors determine the inactive switches of the left and right bridge arms in a 60° interval in the positive and negative half cycles of the output voltage. The inactive interval has a 30° lag from the voltage peak.

DPWM1: V_7 is selected in Sectors 12, 1, 4, 5, 8, and 9. V_0 is selected in the remaining sectors. These vectors determine the inactive switches of the left and right bridge arms in a 60° interval in the positive and negative half cycles of the output voltage. The inactive interval corresponds to the voltage peak.

DPWM3: V_0 is selected in Sectors 12, 1, 4, 5, 8, and 9. V_7 is selected in the remaining sectors. These vectors determine the inactive switches of the left and right bridge arms in a 60° interval in the positive and negative half cycles of the output voltage. The inactive interval is located between the voltage peak and the voltage zero point.

The k values for the different methods are shown in Table 1.

Table 1. k values for different methods

CPWM	
$0 < k < 1$ (when $k=0.5$, is the traditional SVPWM)	
DPWM	
DPWMmax	$k=1$
DPWMmin	$k=0$
DPWM0	$k=0$ in Sectors (1, 2, 5, 6, 9, 10), the other $k=1$
DPWM2	$k=1$ in Sectors (1, 2, 5, 6, 9, 10), the other $k=0$
DPWM1	$k=1$ in Sectors (12, 1, 4, 5, 8, 9), the other $k=0$
DPWM3	$k=0$ in Sectors (12, 1, 4, 5, 8, 9), the other $k=1$

The three-phase reference voltages u_{sa} , u_{sb} , and u_{sc} are given as

$$u_{si} = U_m \cos(\omega t - 2l\pi/3), \quad (4)$$

where $i \in \{a, b, c\}$, $l \in \{1, 2, 3\}$, $U_m = MU_{dc}$ is the amplitude of u_{si} , ω is the angular frequency, and M is the modulation index.

After normalization with U_{dc} , u_{si} can be expressed as u_{ri}

$$u_{ri} = M \cos(\omega t - 2l\pi/3). \quad (5)$$

By defining u_{\max} and u_{\min} as the maximum and minimum values of u_{ri} , respectively, the modulation function of the generalized SVPWM can be expressed as[14]

$$u_{ri}^* = u_{ri} + u_0 \quad i \in \{a, b, c\}. \quad (6)$$

u_{ri}^* is the new reference modulation waveform, which is obtained by adding one zero sequence component u_0 into the original three-phase reference voltage waveform.

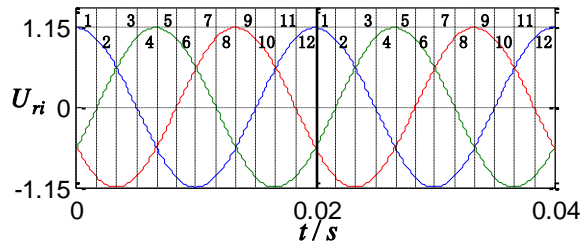
The reference modulation waveform of the different PWM methods can be obtained by different u_0 values, corresponding to different k values. Table 2 shows the correspondence of different k , u_0 , and PWM methods.

As shown in Eq. 6 and Table 2, when $u_0 = 0$ (SPWM), u_0 must satisfy $|u_{ri}^*| = |u_{ri}| \leq 1$, that is, $M \leq 1$. The other PWM methods must satisfy $|u_{ri}^*| = |u_{ri} + u_0| \leq 1$, that is, $M \leq 1.15$. The highest DC voltage utilization ratio of SVPWM is 1.15 times that of SPWM.

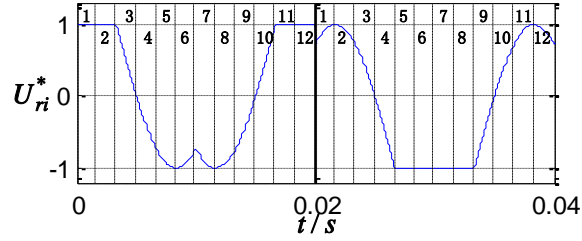
Table 2. Correspondence of different k , u_0 , and PWM methods

SPWM: $u_0 = 0$		
CPWM ($0 < k < 1$)		
$u_0 = (2k - 1) - ku_{\max} - (1 - k)u_{\min}$		
DPWM		
u_0	PWM methods	Constraints
$1 - u_{\max}$	DPWMmax	$k=1$
	DPWM0	$k=1$ (sector S=3,4,7,8,11,12)
	DPWM2	$k=1$ (sector S=1,2,5,6,9,10)
	DPWM1	$k=1$ (sector S=12,1,4,5,8,9)
	DPWM3	$k=1$ (sector S=2,3,6,7,10,11)
$-1 - u_{\min}$	DPWMmin	$k=0$
	DPWM0	$k=0$ (sector S=1,2,5,6,9,10)
	DPWM2	$k=0$ (sector S=3,4,7,8,11,12)
	DPWM1	$k=0$ (sector S=2,3,6,7,10,11)
	DPWM3	$k=0$ (sector S=12,1,4,5,8,9)

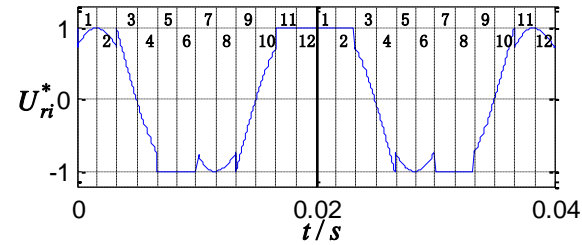
The normalized three-phase reference voltage u_{ri} , the equivalent reference modulation waveform u_{ri}^* , and their corresponding sectors are shown in Figure 3, where the value of the modulation index is $M=1.15$ except in SPWM ($M=1$).



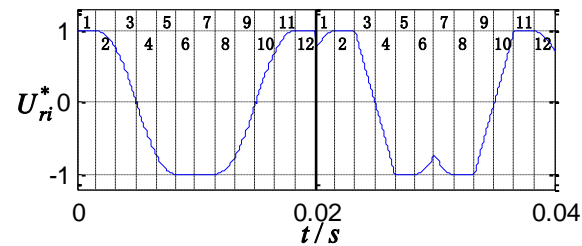
a) u_{ri}



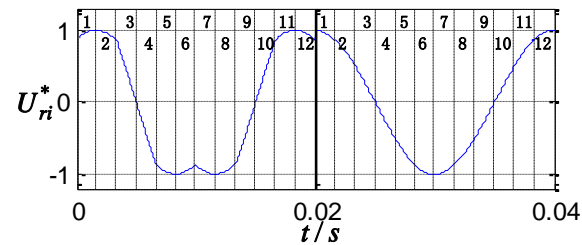
b) DPWMmax c) DPWMmin



d) DPWM0 e) DPWM2



f) DPWM1 g) DPWM3



h) SVPWM i) SPWM

Figure 3. u_{ri} , u_{ri}^* , and their corresponding sectors

As shown in Figure 3, the sectors are obtained by comparing the instantaneous values of u_{ri} . Table 3 shows the specific judgment methods.

Table 3. Sectors judgment

Sectors (S)	judgment methods	
1	$u_{ra} > u_{rb} > u_{rc}$	$u_{rb} < 0$
2		$u_{rb} > 0$
3	$u_{rb} > u_{ra} > u_{rc}$	$u_{ra} > 0$
4		$u_{ra} < 0$
5	$u_{rb} > u_{rc} > u_{ra}$	$u_{rc} < 0$
6		$u_{rc} > 0$
7	$u_{rc} > u_{rb} > u_{ra}$	$u_{rb} > 0$
8		$u_{rb} < 0$
9	$u_{rc} > u_{ra} > u_{rb}$	$u_{ra} < 0$
10		$u_{ra} > 0$
11	$u_{ra} > u_{rc} > u_{rb}$	$u_{rc} > 0$
12		$u_{rc} < 0$

2.2. The generalized SVPWM modulator of a single-stage inverter

The PWM waveform for the left bridge arm is obtained by comparing u_{ri}^* and the triangular carrier with an amplitude of 1. Through unipolar double frequency theory, the PWM waveform for the right bridge arm is obtained by comparing u_{ri}^* with the 180° phase shift and the triangular carrier.

In Phase A, the triangular carrier, the reference modulation waveform of the left and right bridge arms, the switching signals of the upper tube in the left and right bridge arms, and the output waveform of the H-bridge are shown in Figure 4. In the figure, the carrier frequency is $f_c=1/T_s=500$ Hz, and the reference modulation waveform frequency is $f=50$ Hz. The modulation method in Figure 4 is DPWMmin. The generalized SVPWM modulator is shown in Figure 5.

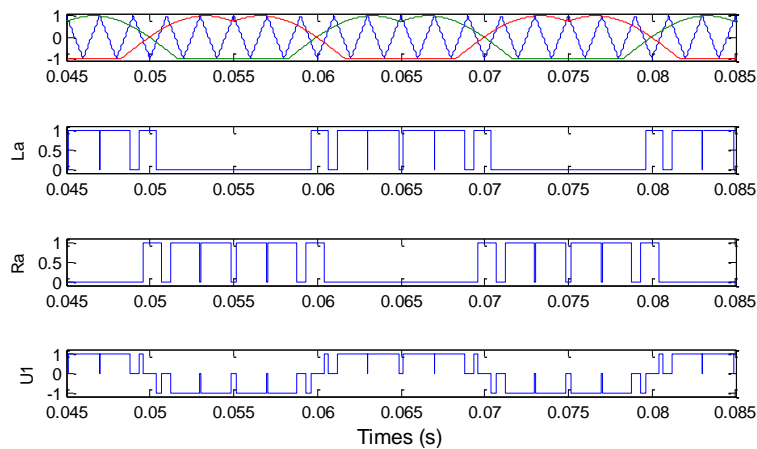


Figure 4. Phase A modulation and switching signals of DPWMmin

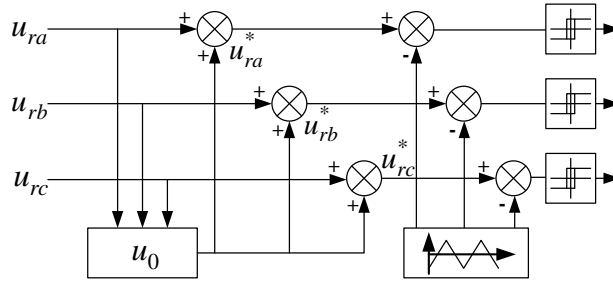


Figure 5. The generalized SVPWM modulator

2.3. PWM of a multilevel inverter

By using the carrier phase shift technique, the carriers of adjacent single-stage inverters deviated by $T_s/2N$, where N is the series of cascaded inverters, and T_s is the carrier cycle. The PWM waveforms of all single-stage inverters are obtained by comparing the carriers and the reference modulation waveforms. The output voltage of each single-stage inverter and the total output voltage of Phase A are shown in Figure 6, where $N=3$, $U_{dc} = 750$ V, $f_c=500$ Hz, and $f=50$ Hz.

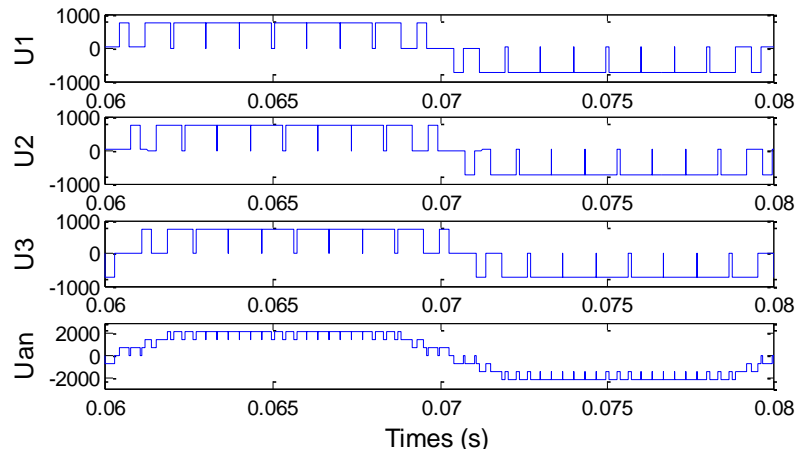


Figure 6. Waveforms of the three cascaded 7-level inverters

2.4. Digital implementation of the generalized SVPWM

PWM waveforms can be simulated in MATLAB/Simulink by the intersection point, which is obtained by comparing the reference modulation waveform and the triangular carrier. In practical applications, one major limitation of the method is the difficulty of its implementation in a digital modulation system. The intersection between the reference modulation waveform and the triangular carrier is defined by a transcendental equation and requires complex calculation [15].

The regular sample PWM waveforms in a single carrier cycle are shown in Figure 7, where T_s is the carrier cycle, u_{ri}^* ($i=a, b, c$) is the reference modulation waveform of the left bridge arm after regular sampling, and T_{cmpLi} ($i=a, b, c$) is the switching pot of the left bridge arm.

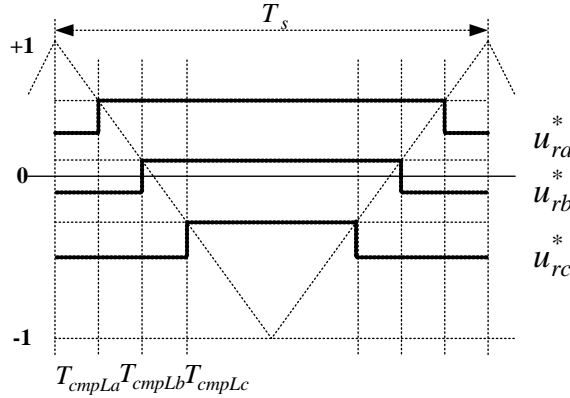


Figure 7. Carrier-based PWM waveforms

We obtain the following equation using the law of similar triangles:

$$\frac{T_{cmpLi}}{T_s/2} = \frac{1-u_{ri}^*}{2}, \quad (7)$$

$$T_{cmpLi} = \frac{T_s(1-u_{ri}^*-u_0)}{4}. \quad (8)$$

The switching pot of the left bridge arm under different PWM methods is shown in Table 4.

Table 4. Switching pot of the left arm under different PWM methods

CPWM ($0 < k < 1$)		
$T_{cmpLi} = -\frac{T_s u_{ri}}{4} + \frac{T_s(2-2k+ku_{max}+(1-k)u_{min})}{4}$		
DPWM		
T_{cmpLi}	PWM methods	Constraints
$-\frac{T_s u_{ri}}{4} + \frac{T_s u_{max}}{4}$	DPWMmax	$k=1$
	DPWM0	$k=1$ (S=3,4,7,8,11,12)
	DPWM2	$k=1$ (S=1,2,5,6,9,10)
	DPWM1	$k=1$ (S=12,1,4,5,8,9)
	DPWM3	$k=1$ (S=2,3,6,7,10,11)
$-\frac{T_s u_{ri}}{4} + \frac{T_s(2+u_{min})}{4}$	DPWMmin	$k=0$
	DPWM0	$k=0$ (S=1,2,5,6,9,10)
	DPWM2	$k=0$ (S=3,4,7,8,11,12)
	DPWM1	$k=0$ (S=2,3,6,7,10,11)
	DPWM3	$k=0$ (S=12,1,4,5,8,9)

The switching pot of the left bridge arm T_{cmpLi} ($i = a, b, c$) is obtained by using Table 4. Similar to traditional SVPWM theory, a single-stage isosceles triangle is selected as the

carrier, where the amplitude is $T_s/2$ and the cycle is T_s . The PWM waveform of the left bridge arm in Sector 1 is shown in Figure 8. The waveform is obtained by comparing T_{cmpLi} and the carrier. The switching pot of the right bridge arm T_{cmpRi} ($i = a, b, c$) is obtained by shifting the reference modulation waveform by 180° .

In the digital modulation system, a timer interrupt can be used. The T_{cmpLi} is sampled in the valley of the triangular carrier, and then, the timer is started. When the timing time is T_{cmpLi} , an interrupt is generated such that the switch signal is set as $L_i=1$, and then, the timer is restarted. When the timing time is $T_s - T_{cmpLi}$, an interrupt is generated such that the switch signal is set as $L_i=0$. The same procedure is performed for the right bridge arm.

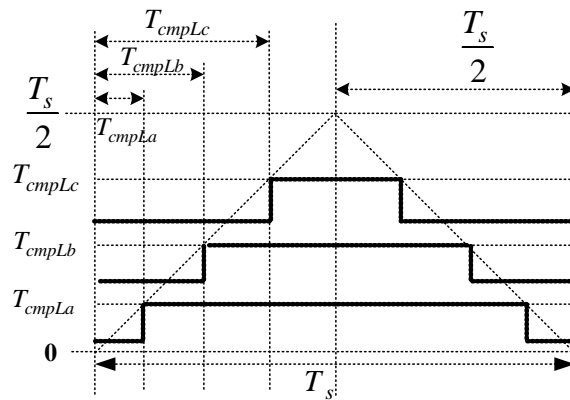


Figure 8. Time-based PWM waveforms

3. Realizing Generalized SVPWM

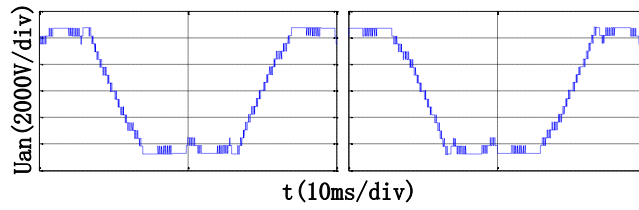
3.1. Experiment platform

To test the feasibility and correctness of the proposed method and to determine if the results are close to actual industrial applications, a 6 KV medium-voltage static synchronous compensator (STATCOM) is investigated. This compensator is one of the reactive power compensation products in the “coal mine power grid safety and energy-saving Xuzhou Engineering Research Center.” The simulation model of the device is built with the same parameters by using MATLAB/Simulink. The parameters are as follows.

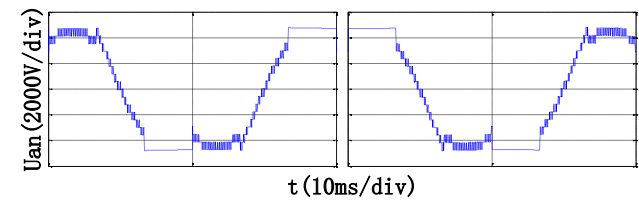
The system rated line virtual voltage is 6 KV. The rated capacity is $S=2.8$ MVar. The rated phase currents are $I=245$ A, $f=50$ Hz, $f_c=500$ Hz, and $U_{dc}=600$ V.

The insulated gate bipolar translator with 1700 V/450 A is selected as the switching device. The STATCOM is connected to the power grid via an LCL filter.

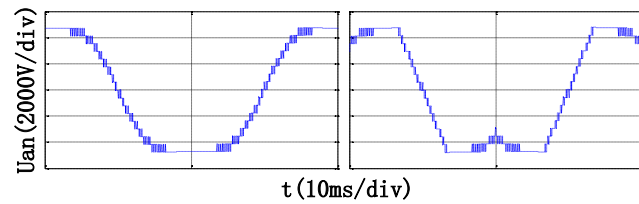
The simulation waveforms are shown in Figure 9, and the experiment waveforms, where the modulation index is $M=1.15$, except for SPWM ($M=1$), are shown in Fig 10.



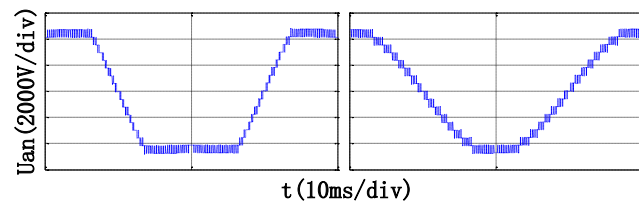
a) DPWMmax b) DPWMmin



c) DPWM0 d) DPWM2



e) DPWM1 f) DPWM3



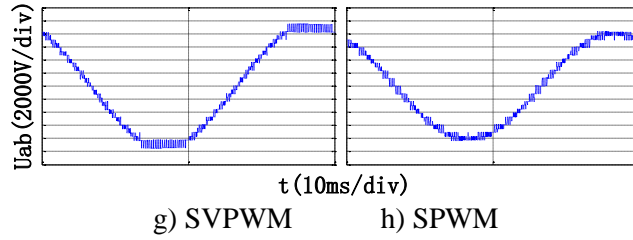


Figure 9. U_{an} and U_{ab} simulation waveforms of different modulation methods

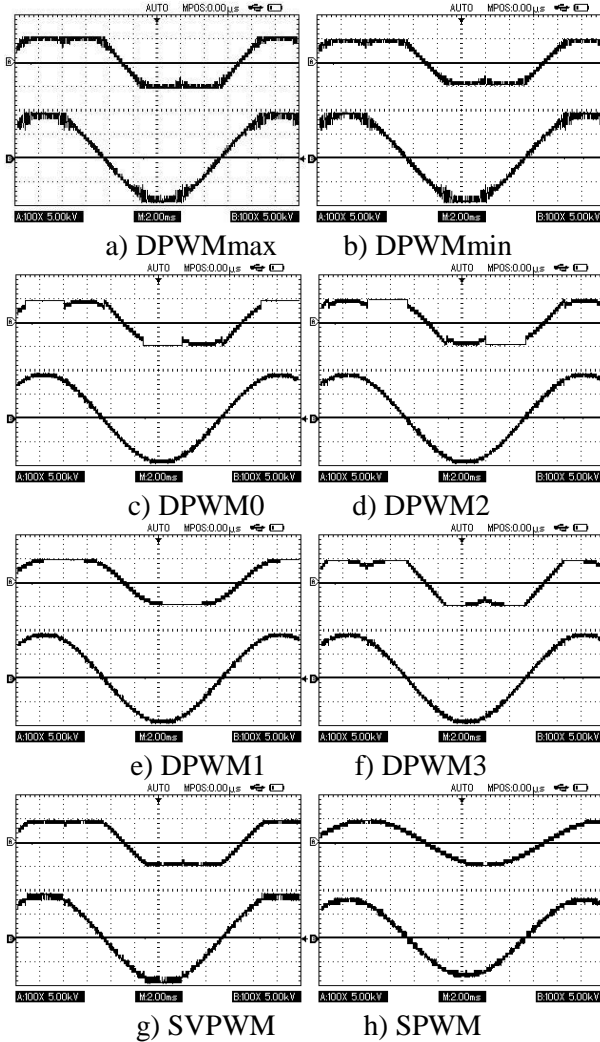


Figure 10. U_{an} and U_{ab} experimental waveforms of different modulation methods

3.2. Harmonic performance analysis

The curves of the total harmonic distortion (THD) factors of the line voltage for different PWM methods within the linear modulation range are shown in Figure 11.

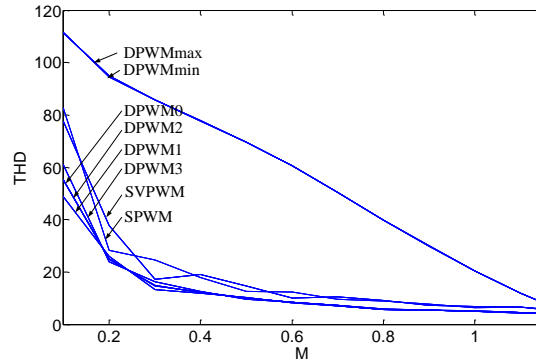


Figure11. The curves of the THD factors for different PWM methods

Table 5 shows the THD and fundamental components of the line voltage for different PWM methods under $M=1$.

Table 5. The THD and fundamental components of the line voltage for different PWM methods under $M=1$

PWM methods	Fundamental component(V)	THD
DPWMmin	8199	20.4%
DPWMmax	8192	20.49%
DPWM0	8195	5.05%
DPWM2	8199	5.03%
DPWM1	8194	5.10%
DPWM3	8199	4.97%
SVPWM	8193	5.6%
SPWM	7117	5.99%

As shown in Figures 9 and 10, the experimental and simulation results are basically identical. The results demonstrate the validity of the generalized SVPWM for cascaded multilevel inverters. Based on Figure 11, the methods of DPWM0, DPWM2, DPWM1, and DPWM3 are better than that of SPWM. The figure also shows that the methods DPWMmax and DPWMmin provide poor line voltage THD compared with those of the other PWM methods. In the DPWM methods, the switch has at least one inactive segment for a total of 120° at maximum. Therefore, the equivalent switching frequency of DPWM is $3/2$ times those of CPWM and SPWM. Table 5 also shows that the highest DC voltage utilization ratios of DPWM and CPWM are 1.15 times that of SPWM

4. Conclusion

In this study, a generalized SVPWM modulator for cascaded H-bridge multilevel inverters is built by using the generalized SVPWM and carrier phase shift methods. Different PWM methods are obtained easily by changing the zero vector distribution coefficient. A simple digital realization method for the generalized SVPWM is proposed.

The simulation and experimental results demonstrate the advantages as follows.

1. Sector judgment is simplified, thus avoiding calculations such as complex trigonometric function calculations, coordinate transformations, and space vector selections.
2. The optimum PWM methods can be determined easily under different loads by changing the k value.
3. The carrier-based SVPWM method can be implemented with digital signal processing hardware.
4. The advantage of the highest DC voltage utilization ratio of traditional SVPWM is inherited.

Acknowledgements

This work was supported by the Research Fund for the Doctoral Program of Higher Education of China under grant 20110095110014 and by the Key (Key grant) Project of Chinese Ministry of Education under grant 311021.

References

- [1] X. Xu, "Research on cascaded multilevel inverter based on STATCOM and its control", Doctoral dissertation of Huazhong University of Science and Technology, (2006).
- [2] R. Naderi and A. Rahmati, "Phase-shifted carrier PWM technique for general cascaded inverters", IEEE Trans. Power Electron, vol. 23, no. 3, (2008), pp. 1257-1269.
- [3] K. C. Jana, S. K. Biswas and P. Thakura, "A simple and generalized space vector PWM control of cascaded H-bridge multilevel inverters", IEEE International conference on digital object identifier, (2006), pp. 1281-1286; Mumbai.
- [4] M. Trabelsi, L. Ben-Brahim, T. Yokoyama, A. Kawamura, R. Kurosawa and T. Yoshino, "An improved SVPWM method for multilevel inverters", Power Electronics and Motion Control Conference, 2012 15th International Digital Object Identifier, (2012), LS5c.1-1 - LS5c.1-7; Novi Sad.
- [5] L. Asiminoaei, P. Rodriguez and F. Blaabjerg, "Application of discontinuous PWM modulation in active power filters", IEEE Trans. Power Electron, vol. 23, no. 4, (2008), pp. 1692-1706.
- [6] N. V. Nguyen, B. X. Nguyen and H. H. Lee, "An optimized discontinuous PWM method to minimize switching loss for multilevel inverters", IEEE Trans. Ind. Electron, vol. 58, no. 9, (2011), pp. 3958-3966.
- [7] F. Yu, X. Zhang, H. Li and Y. Liu, "A zero sequence offset time based low loss and high performance PWM method", Automation of Electric Power System, vol. 29, no. 2, (2005), pp. 39-44.
- [8] O. Ojo, "The generalized discontinuous PWM scheme for three-phase voltage source inverters", IEEE Transactions on Industrial Electronics, vol. 51, no. 6, (2004), pp. 1280-1289.
- [9] F. Ma, Z. Wu and X. Hou, "Random Space Vector PWM based on the Generalized Modulator", Proceeding of the CSEE, vol. 27, no. 7, (2007), pp. 98-102.
- [10] X. Wen, X. Yin and Z. Zhang, "Unified Space Vector PWM Implementation Method for Three-Phase Inverters", Transactions of China Electrotechnical Society, vol. 24, no. 10, (2009), pp. 87-93.
- [11] Z. Shi and X. Shi, "A Novel Technique of SVPWM Based on Cascaded H-Bridge Multi-level Inverter", Transactions of China Electrotechnical Society, vol. 20, no. 10, (2005), pp. 30-97.
- [12] B. Huang, L. Xia and Z. Wu, "Research of Phase-Shifted SVPWM Based on H-Bridge Cascaded Multilevel Inverter", Telecom Power Technology, vol. 28, no. 3, (2011), pp. 21-24.
- [13] L. Wei, K. Jin and M. Wang, "The research and implementation of a novel SVPWM modulation method", Electrical Measurement & Instrumentation, vol. 47, no. 532, (2010), pp. 9-12.
- [14] J. Kolar, H. Ertl and F. Zach, "Influence of the modulation method on the conduction and switching losses of a PWM converter system", IEEE Transactions on Industry Application, vol. 27, no. 6, (1991), pp. 1063-1075.
- [15] D. G. Holmes and T. A. Lipo, "Pulse width modulation for power converters: principles and practice", Wiley-IEEE Press, (2003).

Authors



Xiaodong YANG. He is currently pursuing the doctorate in power electronics and power transmission at China University of Mining and Technology(CUMT), China. He received his MS degree in Information and Electrical Engineering from CUMT in 2008, and his BS degree in Information and Electrical Engineering from CUMT in 2005. He is currently a student at School of Information and Electrical Engineering, CUMT. His research interests are fault diagnosis and fault-tolerant control of power electronics.



Chonglin Wang. He is born in 1956, Ph.D. He is a professor at School of Information and Electrical Engineering in CUMT. His research interests are electrical safety and intelligent electrical apparatus. He has published more than 60 research papers in journals and international conferences.



Liping Shi. She is born in 1964, Ph.D. She is a professor at School of Information and Electrical Engineering in CUMT. Her research interests are coal mine mechanical and electrical equipment and automation, application of power electronics in power systems, and equipment and power grid operation and fault diagnosis. She has published more than 30 research papers in journals and international conferences and she has won more than 10 the provincial scientific research awards.



Zhenglong Xia. He is current a Ph.D.candidate at China University of Mining and Technology(CUMT), China. He received her MS degree in Information and Electrical Engineering from CUMT in 2008, and her BS degree in Information and Electrical Engineering from CUMT in 2005. He is currently a student at School of Information and Electrical Engineering, CUMT. His research interests are reactive compensation of power system, fault diagnosis, distributed parallel processing, and neural network.

